Electric dipole moment of ^{225}Ra due to P- and T-violating weak interactions

Yashpal Singh* and B. K. Sahoo†

Theoretical Physics Division, Physical Research Laboratory, Navrangpura, Ahmedabad 380009, India

(Received 27 April 2015; published 6 August 2015)

Employing advanced methods in the relativistic coupled-cluster framework, the electric dipole moments (EDM) of ^{225}Ra due to parity- and time-reversal-violating tensor-pseudotensor (T-PT) and nuclear Schiff moment (NSM) interactions are obtained as $d_A = -10.01 \times 10^{-20} C_T \langle \sigma_n \rangle |e|$ cm and $d_A = -6.79 \times 10^{-17} S(|e|\text{fm}^3)^{-1}|e|$ cm, respectively, with C_T being the T-PT coupling constant and S being NSM. These values for the corresponding T-PT and NSM interactions are reduced by about 45% and 23%, respectively, compared to the previous calculations. The validity of our calculations is proved by comparing our results with the earlier studies using the zeroth-order Dirac-Fock method and all-order random-phase approximation. The first measurement of ^{225}Ra EDM was reported recently [R. H. Parker *et al.*, Phys. Rev. Lett. **114**, 233002 (2015)], and in that study the authors also anticipate obtaining the result with an improvement in systematics and the statistical sensitivity of the experiment, which could possibly lead to the best limit for an atomic EDM. Thus, it offers considerable hope to extract more accurate limits for the electron-quark T-PT interaction and the θ_{QCD} parameter in particle physics in the future.

DOI: 10.1103/PhysRevA.92.022502 PACS number(s): 31.30.jp, 11.30.Er, 24.80.+y, 31.15.ve

An experimental group at Argonne National Laboratory (ANL) has recently announced its first measurement of the permanent electric dipole moment (EDM) of ^{225}Ra [1] after making steady progress in the last several years [2–4]. The upper limit they obtained for the atomic EDM d_A is $|d_A(^{225}\text{Ra})| < 5.0 \times 10^{-22}|e|$ cm (at 95% confidence). Although this is not competitive with the current best limit available from ^{199}Hg [5], which is $|d_A(^{199}\text{Hg})| < 3.1 \times 10^{-29}|e|$ cm (at the same 95% confidence level), the ongoing measurement of the Ra EDM at ANL promises to yield a limit which could surpass that obtained from ^{199}Hg in the future [1]. In fact, this seems likely from both theoretical and experimental considerations. From the theoretical point of view, the octupole deformation in the nucleus of ^{225}Ra can enhance EDM by two to three orders of magnitude compared to ^{199}Hg [6,7]. The other prominent theoretical advantages favoring the observation of the ^{225}Ra EDM are that this atom has a larger nuclear charge than ^{199}Hg and, like ^{199}Hg, it has nuclear spin $I = 1/2$, due to which the contributions from the octupole moment vanish. On the experimental front, cold-atom techniques with very little sensitivity to systematics [8] have been developed to measure the Larmor spin-resonance frequency for ^{225}Ra atoms [2,4]. Moreover, using the Facility for Rare Isotope Beams (FRIB) for a measurement time of 100 days, the ANL research group hopes to bring about a significant improvement in the statistical uncertainty by increasing the number of atoms that can be observed to 10^6 [1].

The EDM of a diamagnetic atom like ^{225}Ra is sensitive to the parity (P) and time-reversal (T) violating (P,T-odd) electron-nucleon tensor-pseudotensor (T-PT) and nuclear Schiff moment (NSM) interactions. The NSM originates primarily from the distorted charge distribution inside the nucleus caused by the P,T-odd interactions among the nucleons or from the EDMs and chromo-EDMs of the up ($\tilde{d}_u$) and down ($\tilde{d}_d$) quarks [9]. Thus, the existence of a nonzero EDM is a clear signature of violation of the P and T symmetries. T violation implies CP violation as a consequence of the CPT theorem. All the observed CP violations to date are consistent with the standard model (SM) of particle physics [10,11], but the SM fails to explain the observed finite-neutrino masses, the matter-antimatter asymmetry in the universe, the existence of dark matter, etc. [12,13]. To answer these profound questions many extensions of the SM, such as the multi-Higgs, supersymmetry, and left-right symmetric models, have been propounded [14–16]. These extensions envision additional CP-violating couplings which magnify the EDMs of the elementary particles, thereby resulting in large EDMs in atoms. The NSM at the fundamental level is related to the θ_{QCD} parameter of particle physics, and possibly, a large value of θ_{QCD} would point to new sources of CP violation, apart from the δ phase of the SM [14,17]. Thus, accurate estimates of the upper limits on the T-PT coupling coefficient and the NSM of an atom could help to explain new physics and may probe the efficacy of certain beyond-SM models. Consequently, ongoing efforts to improve limits on the extracted parameters from the atomic EDMs, even with null results, are still valuable.

The limit on the ^{225}Ra EDM is anticipated to supersede that obtained from ^{199}Hg EDM [1]. It is therefore now imperative to perform the corresponding calculations accurately so that in combination with the improved measurement, better limits on the above-mentioned parameters can be obtained. We employ here relativistic many-body methods in different forms at various approximations [17–19] to determine very accurately d_A for ^{225}Ra arising due to both the T-PT (d_A^{TPT}) and NSM (d_A^{NSM}) interactions. We find that the correlation effects in the calculations of these properties are remarkably large, as a result of which the final results are reduced substantially compared to the values reported earlier [20–22]. In order to demonstrate the validity of our methods, we present the results from the intermediate Dirac-Fock (DF) method and random-phase approximation (RPA) to cross-check the consistencies of these values with the previous calculations. We improve the accuracies of our calculations by incorporating more physical effects (specifically, the non-RPA correlations) systematically through the coupled-cluster (CC) method at different levels of truncation. We also evaluate the dipole polarizability α_d of

*yashpal@prl.res.in
†bijaya@prl.res.in

^{225}Ra to compare its value with the other CC calculation [23] to ensure the reliability of our method.

The electron-nucleus (e-N) interaction Hamiltonians due to T-PT coupling and NSM are given by [24,25]

$$H_{e-N}^{T-PT} = \frac{iG_F C_T}{\sqrt{2}} \sum \vec{\sigma}_n \cdot \vec{\gamma}_D \rho_n(r), \tag{1}$$

$$H_{e-N}^{\rm NSM} = \frac{3\vec{S}\cdot\vec{r}}{B_4}\rho_n(r), \tag{2}$$

respectively, where G_F is the Fermi constant, C_T is the T-PT coupling constant, $\vec{\sigma}_n = \langle\sigma_n\rangle\vec{\mathbf{I}}/I$ is the Pauli spinor of the nucleus, $\vec{\gamma}_D$ represents the Dirac matrices, $\rho_n(r)$ is the nuclear charge density, $\vec{S} = S\vec{\mathbf{I}}/I$ is the NSM, and $B_4 = \int_0^\infty dr r^4 \rho_n(r)$.

In our calculations, we first obtain the DF wave function $|\Phi_0\rangle$ for the ground state of ^{225}Ra using the Dirac-Coulomb (DC) atomic Hamiltonian $H_{\rm DC}$. Considering $|\Phi_0\rangle$ the reference state, the exact state $|\Psi_0\rangle$ is determined by appending the electron correlations in the second-order and third-order many-body perturbation theory [denoted by MBPT(2) and MBPT(3) respectively], RPA, and CC methods. Detailed formulations of these methods are explained and employed in our previous works [17–19,26]. For the reader's sake, a brief description of our CC method at various levels of approximation is given here. The first-order correction to the CC wave function $|\Psi_0^{(0)}\rangle = e^{T^{(0)}}|\Phi_0\rangle$, with $T^{(0)}$ being the excitation operator, for the evaluation of d_A and α_d with the respective P,T-odd interaction Hamiltonians and the $E1$ operator D is expressed as [17–19,26]

$$\left|\Psi_0^{(1)}\right\rangle = e^{T^{(0)}} T^{(1)}|\Phi_0\rangle, \tag{3}$$

where $T^{(1)}$ is a CC operator similar to $T^{(0)}$ but can generate only the odd-parity excitations acting upon $|\Phi_0\rangle$. For the calculations of both $|\Psi_0^{(0)}\rangle$ and $|\Psi_0^{(1)}\rangle$, we only allow all possible single and double excitations ($T^{(0)} = T_1^{(0)} + T_2^{(0)}$ and $T^{(1)} = T_1^{(1)} + T_2^{(1)}$) in the CC method (known as CCSD). We also consider contributions from the important triple excitations perturbatively through the singles, doubles, and partial triples CC [CCSD(T)] method as explained in [17]. To substantiate the notable roles of the nonlinear CC terms, we also determine properties considering only the linear terms in the CCSD (referred to as LCCSD) method. The nonlinear terms virtually conform with the triples, quadruples, etc., excitations. In the CC approach, both d_A and α_d (commonly denoted as $\mathcal{X}$) are evaluated by [17–19]

$$\mathcal{X} = 2\langle\Phi_0|(\overline{D}^{(0)}T^{(1)})_{cc}|\Phi_0\rangle, \tag{4}$$

where cc stands for the closed and connected terms and $\overline{D}^{(0)} = e^{T^{\dagger(0)}} D e^{T^{(0)}}$. In our previous work [17], we have described the procedure by which we take into account contributions from the above nontruncative series in an iterative procedure. We also present intermediate CCSD results as CCSD$^{(k)}$, truncating the series with intermediate $k = 2,4,\ldots$ degree nonlinear terms to highlight the relevance of the higher-power terms in the accurate determination of d_A and α_d (note that CCSD without the suffix k refers to CCSD$^{(\infty)}$).

TABLE I. Comparison of α_d, $d_A^{\rm TPT}$, and $d_A^{\rm NSM}$ (in ea_0^3, $10^{-20}\, C_T\,\langle\sigma_n\rangle|e|$ cm, and $10^{-17}\,[S/|e|\,\text{fm}^3]|e|$ cm, respectively) results for ^{225}Ra from various calculations. The CCSD(T) results are the converged values from our calculations, and the RPA values for the Breit interaction (δ_B), QED correction ($\delta_{\rm QED}$), and truncated basis ($\delta_{\rm basis}$) are given at the end.

Method of evaluation	This work			Other studies		
	α_d	$d_A^{\rm TPT}$	$d_A^{\rm NSM}$	α_d	$d_A^{\rm TPT}$	$d_A^{\rm NSM}$
DF	204.13	−3.46	−1.85	204.2[a]	−3.5[a]	−1.8[a]
				200.6[b]		
				293.4[c]		
MBPT(2)	230.67	−11.00	−5.48			
MBPT(3)	189.53	−10.59	−5.30			
RPA	296.85	−16.66	−8.12		−17[a]	−8.3[a]
				291.4[b]	−16.59[b]	
				297.0[d]		−8.5[d]
CI + MBPT					−18[a]	−8.8[a]
				229.9[d]		
LCCSD	251.88	−13.84	−8.40			
CCSD$^{(2)}$	253.04	−10.40	−6.94			
CCSD$^{(4)}$	242.02	−9.49	−6.52			
CCSD$^{(\infty)}$	247.76	−10.04	−6.79	251.8[c]		
CCSD(T)	241.40	−10.01	−6.79	242.8[c]		
δ_B	0.19	0.06	0.06			
$\delta_{\rm QED}$	−0.43	−0.16	−0.07			
$\delta_{\rm basis}$	−0.03	−0.08	−0.05			

[a]Reference [21].
[b]Reference [22].
[c]Reference [23]. Corrections from the Gaunt term are incorporated.
[d]Reference [20]. Corrections from RPA are included.

Results for α_d, $d_A^{\rm TPT}$, and $d_A^{\rm NSM}$ of ^{225}Ra using the considered methods are given in Table I. We also give the previously reported results from different methods for comparison. Among these, calculations using the combined configuration interaction and leading-order many-body perturbation theory (CI + MBPT method) with some corrections through the time-dependent Hartree-Fock method (equivalent to our RPA) by Dzuba and coworkers [20,21] were presumed to be more rigorous. This approach, however, uses a V^{N-2} potential ($N = 88$ is the total number of electrons of ^{225}Ra) to generate the single-particle orbitals, in contrast to our V^N potential. Unlike our methods, this hybrid method cannot include the correlation effects from all the electrons on equal footing, which is essential for a strongly interacting atom like ^{225}Ra. In fact, Dzuba and coworkers [20,21] and Latha and Amjith [22] have independently employed RPA with the V^N potential to report d_A and α_d. From the comparison in Table I, we find that the DF and RPA results, among all these calculations, agree quite well with each other. α_d is often evaluated together with d_A and compared with its experimental value because the same angular momentum and parity selection criteria are required for their determination, notwithstanding their different radial behavior, to test the potential of the method [17–22]. The experimental result of α_d in ^{225}Ra is yet to be realized, but a few calculations using variants of the CC methods report its value, among which the latest calculations by Borschevsky

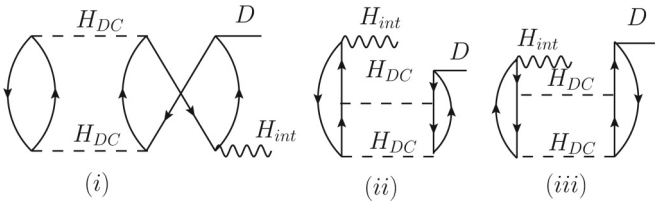

FIG. 1. A few important non-RPA diagrams from the MBPT(3) method. Lines with up and down arrows are the occupied and unoccupied orbitals, respectively. $H_{\rm int}$ corresponds to either H_{e-N}^{T-PT}, $H_{e-N}^{\rm NSM}$, or D operators in the evaluation of $d_A^{\rm TPT}$, $d_A^{\rm NSM}$, and α_d, respectively.

et al. present DF, CCSD, and CCSD(T) results [23] and make a comparative analysis with the previous calculations. They use the DC Hamiltonian with the Gaunt term in a finite-field approach and get a large DF value, whereas their CC results, as seen in Table I, converges towards a value similar to our CC results.

We also estimate the order of magnitude of the neglected effects, such as corrections due to the truncated basis ($\delta_{\rm basis}$), Breit interaction (δ_B), and quantum electrodynamic (QED) effects ($\delta_{\rm QED}$), in our calculations by using RPA in a manner similar to that in our previous work [19]. These values are given at the end of Table I. Assuming differences between the CCSD(T) and CCSD results from our calculations are the largest possible contributions from the omitted higher-level excitations and the above corrections, our CCSD(T) results are estimated to have uncertainties less than 2%.

The present study also highlights that the behavior of electron correlation effects in ^{225}Ra is different from other closed-shell atoms such as ^{129}Xe [18], ^{223}Rn [19], and ^{199}Hg [17] for the EDM studies. For example, RPA estimates EDMs within reasonable accuracies in ^{129}Xe [18] and ^{223}Rn [19], while the CCSD method and the CI + MBPT approach of Dzuba and coworkers give almost similar results for ^{199}Hg [17]. As seen from Table I, the CCSD(T) values for α_d, $d_A^{\rm TPT}$, and $d_A^{\rm NSM}$ distinctly differ by 5% (increased), 45% (reduced), and 23% (reduced), respectively, from the CI + MBPT results in ^{225}Ra. The main reason for these large differences is the significant non-RPA and core correlation contributions in the considered properties. This is apparent from the differences between the MBPT(2) and MBPT(3) results and the LCCSD and CCSD$^{(2)}$ results given in Table I since MBPT(2) corresponds to the lower-order RPA, whereas the non-RPA contributions start appearing in MBPT(3). For quantitative substantiation, we present a few important non-RPA contributions (depicted diagrammatically in Fig. 1) from MBPT(3) in Table II. We also

TABLE II. Non-RPA contributions from the MBPT(3) diagrams shown in Fig. 1 along with their exchange parts. The units for α_d, $d_A^{\rm TPT}$, and $d_A^{\rm NSM}$ are the same as in Table I.

	Contributions		
	α_d	$d_A^{\rm TPT}$	$d_A^{\rm NSM}$
Diagram (i)	−52.19	2.01	0.97
Diagram (ii)	−25.98	1.29	0.62
Diagram (iii)	−14.77	0.49	0.20

TABLE III. Individual contributions to α_d, $d_A^{\rm TPT}$, and $d_A^{\rm NSM}$ (same units as in Table I) from various LCCSD, CCSD, and CCSD(T) terms arising in Eq. (4). "Extra" corresponds to the leftover terms.

Method	$DT_1^{(1)}$	$T_1^{(0)\dagger}DT_1^{(1)}$	$T_2^{(0)\dagger}DT_1^{(1)}$	$T_2^{(0)\dagger}DT_2^{(1)}$	Extra
			α_d (ea_0^3)		
LCCSD	277.57	−22.09	−30.17	24.17	2.40
CCSD	273.09	−20.14	−32.83	30.60	−2.96
CCSD(T)	269.08	−22.60	−30.47	30.19	−2.80
			$d_A^{\rm TPT}$ $(10^{-20}\, C_T \langle\sigma_n\rangle |e|$ cm)		
LCCSD	−16.62	0.01	3.54	−0.41	−0.36
CCSD	−13.37	−0.08	3.32	−0.19	0.28
CCSD(T)	−13.34	−0.09	3.33	−0.20	0.29
			$d_A^{\rm NSM}$ $(10^{-17}\, [S/|e|\,{\rm fm}^3] |e|$ cm)		
LCCSD	−9.37	0.06	1.63	−0.75	0.03
CCSD	−7.76	0.02	1.59	−0.83	0.19
CCSD(T)	−7.77	0.02	1.59	−0.83	0.21

give the contributions from the LCCSD, CCSD, and CCSD(T) methods in Table III to affirm the importance of different electronic configurations in the accurate evaluation of the above properties. As seen, $DT_1^{(1)}$ yields the largest contributions in all the cases, alluding to careful inclusion of the singly excited configurations in the calculations for achieving accurate results in ^{225}Ra. Nevertheless, doubly excited contributions through $T_2^{(1)}$ are also found to be crucial. Comparing the LCCSD and CCSD(T) results, we observe that singly excited amplitudes are modulated in the calculation of d_A, while the doubly excited amplitudes are altered substantially in the evaluation of α_d. We also investigate proportionate contributions to $DT^{(1)}$ in the CCSD(T) method from different matrix elements of the P,T-odd interaction Hamiltonians and $E1$ operator between the core and virtual orbitals; the dominant matrix element contributions to α_d and d_A are shown as histograms in Fig. 2. This figure clearly exhibits uneven contributions to α_d, $d_A^{\rm TPT}$, and $d_A^{\rm NSM}$ from different matrix elements between the low-lying orbitals of ^{225}Ra.

Combining our CCSD(T) result for $d_A^{\rm NSM}$ with the measured d_A (^{225}Ra) value [1], we get an upper bound on NSM as $S < 7.4 \times 10^{-6}\, |e|\,{\rm fm}^3$. Similarly, with the knowledge of $\langle\sigma_n\rangle$ in ^{225}Ra from nuclear calculation, an upper bound on C_T can be predicted. Two sophisticated nuclear calculations have been carried out using the octupole deformed Woods-Saxon potential [7] and odd-A Skyrme mean-field theory [27] to describe the P,T-odd interactions in ^{225}Ra in terms of the pion-nucleon-nucleon (πNN) couplings. In a recent review, Engel *et al.* gave the best value for S from these two calculations as [28]

$$S = 13.5[-1.5\bar{g}_0 + 6.0\bar{g}_1 - 4.0\bar{g}_2]\, |e|\,{\rm fm}^3, \qquad (5)$$

where $\bar{g}_{i=0,1,2}$ are the isospin components of the P,T-odd πNN coupling constants. We infer bounds as $|\bar{g}_0| < 3.6 \times 10^{-7}$ and $|\bar{g}_1| < 9.1 \times 10^{-8}$ using the above result with our extracted limit on S. Again, from the relations $|\bar{g}_0| = 0.018(7)\theta_{QCD}$ [29] and $|\bar{g}_1| = 2 \times 10^{-12}(\tilde{d}_u - \tilde{d}_d)$ [30], we put the upper limits as $|\theta_{QCD}| < 2.0 \times 10^{-5}$ and $|\tilde{d}_u - \tilde{d}_d| < 4.6 \times 10^{-22}\, |e|$ cm. Although at present these bounds are not competitive with the corresponding limits acquired from the

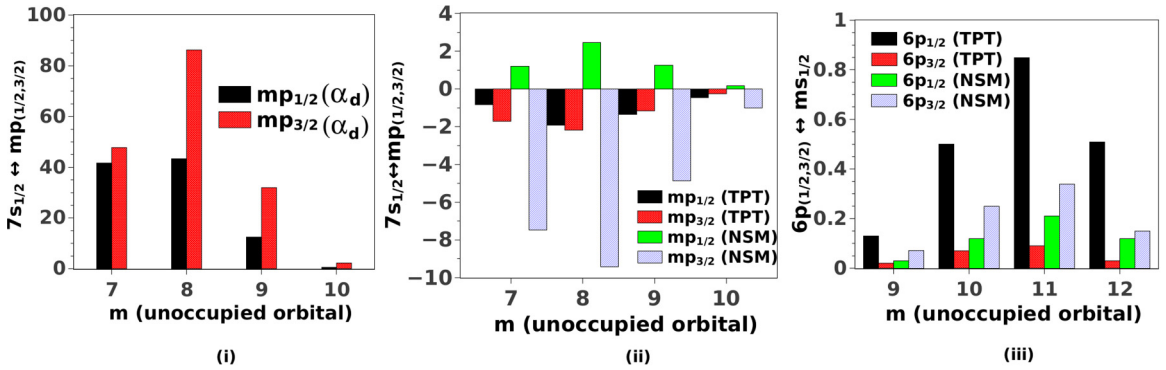

FIG. 2. (Color online) Histograms representing the dominant matrix elements between the $7s$ and $6p$ occupied orbitals and the low-lying virtual ms and mp orbitals, with m being the corresponding principle quantum number, of $DT^{(1)}$ in the CCSD(T) method. Plots for (i) α_d, (ii) the $7s \leftrightarrow mp$ matrix elements of d_A, and (iii) the $6p \leftrightarrow ms$ matrix elements of d_A.

^{199}Hg EDM study [17], the limits could become more stringent when our results are combined with the anticipated improved ^{225}Ra EDM measurement.

We thank Professor B. P. Das for encouraging us to carry out this study. The computations were carried out using 3TFLOP HPC cluster of PRL, Ahmedabad.

[1] R. H. Parker *et al.*, Phys. Rev. Lett. **114**, 233002 (2015).
[2] J. R. Guest, N. D. Scielzo, I. Ahmad, K. Bailey, J. P. Greene, R. J. Holt, Z.-T. Lu, T. P. O'Connor, and D. H. Potterveld, Phys. Rev. Lett. **98**, 093001 (2007).
[3] N. D. Scielzo, J. R. Guest, E. C. Schulte, I. Ahmad, K. Bailey, D. L. Bowers, R. J. Holt, Z.-T. Lu, T. P. O'Connor, and D. H. Potterveld, Phys. Rev. A **73**, 010501(R) (2006).
[4] R. H. Parker *et al.*, Phys. Rev. C **86**, 065503 (2012).
[5] W. C. Griffith, M. D. Swallows, T. H. Loftus, M. V. Romalis, B. R. Heckel, and E. N. Fortson, Phys. Rev. Lett. **102**, 101601 (2009).
[6] N. Auerbach, V. V. Flambaum, and V. Spevak, Phys. Rev. Lett. **76**, 4316 (1996).
[7] V. Spevak, N. Auerbach, and V. V. Flambaum, Phys. Rev. C **56**, 1357 (1997).
[8] M. V. Romalis and E. N. Fortson, Phys. Rev. A **59**, 4547 (1999).
[9] I. B. Khriplovich and S. K. Lamoreaux, *CP Violation without Strangeness: Electric Dipole Moments of Particles, Atoms, and Molecules* (Springer, Berlin, 1997).
[10] J. H. Christenson, J. W. Cronin, V. L. Fitch, and R. Turlay, Phys. Rev. Lett. **13**, 138 (1964).
[11] E. Áavarez and A. Szynkman, Mod. Phys. Lett. A **23**, 2085 (2008).
[12] M. Dine and A. Kusenko, Rev. Mod. Phys. **76**, 1 (2003).
[13] L. Canetti, M. Drewes, and M. Shaposhnikov, New J. Phys. **14**, 095012 (2012).
[14] M. Pospelov and A. Ritz, Ann. Phys. (N.Y.) **318**, 119 (2005).
[15] V. V. Flambaum and J. S. M. Ginges, Phys. Rev. A **72**, 052115 (2005).
[16] T. Fukuyama, Int. J. Mod. Phys. A **27**, 1230015 (2012).
[17] Y. Singh and B. K. Sahoo, Phys. Rev. A **91**, 030501(R) (2015).
[18] Y. Singh, B. K. Sahoo, and B. P. Das, Phys. Rev. A **89**, 030502(R) (2014).
[19] B. K. Sahoo, Y. Singh, and B. P. Das, Phys. Rev. A **90**, 050501(R) (2014).
[20] V. A. Dzuba, V. V. Flambaum, J. S. M. Ginges, and M. G. Kozlov, Phys. Rev. A **66**, 012111 (2002).
[21] V. A. Dzuba, V. V. Flambaum, and S. G. Porsev, Phys. Rev. A **80**, 032120 (2009).
[22] K. V. P. Latha and P. R. Amjith, Phys. Rev. A **87**, 022509 (2013).
[23] A. Borschevsky, V. Pershina, E. Eliav, and U. Kaldor, Phys. Rev. A **87**, 022502 (2013).
[24] A. M. Maartensson-Pendrill, Phys. Rev. Lett. **54**, 1153 (1985).
[25] V. V. Flambaum, I. B. Khriplovich, and O. P. Sushkov, Nucl. Phys. A **449**, 750 (1986).
[26] Y. Singh, B. K. Sahoo, and B. P. Das, Phys. Rev. A **88**, 062504 (2013).
[27] J. Dobaczewski and J. Engel, Phys. Rev. Lett. **94**, 232502 (2005).
[28] J. Engel, M. J. Ramsey-Musolf, and U. van Kolck, Prog. Part. Nucl. Phys. **71**, 21 (2013).
[29] W. Dekens, J. De Vries, J. Bsaisou, W. Bemreuther, C. Hanhart, Ulf-G. Meißner, A. Nogga, and A. Wirzba, J. High Energy Phys. 07 (2014) 069.
[30] M. Pospelov, Phys. Lett. B **530**, 123 (2002).